Magnetic structures in substituted ferrites

1990 J. Phys.: Condens. Matter 2 1223

(http://iopscience.iop.org/0953-8984/2/5/014)

J. Phys.: Condens. Matter **2** (1990) 1223–1237. Printed in the UK

Magnetic structures of substituted ferrites

J L Dormann and M Nogues
Laboratoire de Magnétisme, CNRS, 92195 Meudon Cédex, France

Received 20 July 1989

Abstract. In this paper the magnetic structures of various substituted ferrites are reviewed. Attention is focused on the more usual case of a local canted state. Several systems and detailed magnetic experiments are listed and discussed. Then experimental phase diagrams (tetrahedral–octahedral iron conentrations) are established to distinguish between different magnetic regions: ferrimagnetic order, local canted state or perturbed magnetic order, spin-glass-like phase and in between intermediate regions.

1. Introduction

Very soon after the explanation of the ferrite magnetic moment in terms of the Néel two-sublattice model of ferrimagnetism, it was found that ferrites which had been sufficiently substituted with non-magnetic atoms showed significant departures from the Néel collinear model [1]. Three theoretical models have been used to explain these departures:

(i) a paramagnetic centre model in which the number of magnetic nearest neighbours determines whether a magnetic ion remains paramagnetic or contributes to the magnetisation [2],

(ii) a uniform spin canting relative to the average magnetisation [3] and

(iii) a localised canting where the canting angle of a magnetic ion spin depends on the local magnetic environment [4].

For the latter case attempts [5, 6] have been made to determine mathematical formulae; the calculations in [6] have been refined by several workers [7–9]. Recent reviews on this topic are to be found in [9, 10].

In the last 15 years, several concepts have been developed in order to understand the properties of spin glasses and other disordered magnetic phases. Frustration [11] and randomness are necessary to obtain these types of magnetic phase and are evidently present in substituted ferrites. Generally, the three exchange integrals J_{ab}, J_{bb} and J_{aa} are negative with $|J_{ab}| \gg |J_{bb}|$ and $|J_{aa}|$. Therefore the two magnetic sublattices are antiparallel and J_{aa} and J_{bb} are frustrated. In addition, the substitution of non-magnetic (or magnetic) atoms is always in random positions except in very special cases. For the spinel systems, a model has been developed [12] which leads not only to a spin-glass phase for certain concentrations but also to a new magnetic phase called a semi-spin

0953-8984/90/051223 + 15 $03.50

glass where two transitions are expected: the first at a high temperature for the longitudinal spin component which orders ferrimagnetically, and the second at a low temperature for the transverse spin component which has a spin-glass-type order. The re-entrant state, predicted in [13] from mean-field theory, is phenomenologically strictly equivalent to the semi-spin-glass state.

Bond percolation is another interesting concept. Applied to spinels [14–16], it leads to three regions in the magnetic ion concentration diagram:

(i) a region corresponding to the absence of percolation of intra-sublattice and inter-sublattice bonds which probably leads to paramagnetism;

(ii) another region where the percolation of AB bonds only (neglecting the intra-sublattice bonds) is effective, leading to ferrimagnetism, at least on an average (canted structures can occur in this region);

(iii) finally, an intermediate region between regions (i) and (ii), where disordered magnetic phases are expected such as spin-glass or spin-glass-like phases.

Also, the problem of random uniaxial anisotropy has been studied in order to understand the magnetic properties of amorphous materials containing anisotropic rare earths. Several new magnetic states are predicted depending on the strength of the anisotropy relative to the exchange [17, 18]. Unfortunately, the application of models has not been attempted in the case of spinels where anisotropic Fe^{2+}, Co^{2+} and Mn^{3+} ions can occur in random positions. We discuss, in § 3 of this paper, the possible effect of anisotropic ion substitution on the magnetic structure.

Theoretical studies and very numerous experimental studies performed on various systems have led to the definition of the spin-glass state characterised in particular by a true thermodynamic phase transition occurring at a well defined temperature (for reviews on spin glasses see [19]). It has also been shown that various compounds present some properties similar to those of spin glasses, but cannot be considered as spin glasses because certain crucial properties are not found. The natures of the disordered magnetic states, which are intermediate between the 'true' spin-glass state and classical order, are still not well known (this question is reviewed in [20] and an excellent review on non-collinear spin structure can be found in [21]).

The case of systems with two magnetic sublattices is particularly interesting because they have been the object of intensive experimental studies (ferrites) and they can exhibit at least one particular disordered magnetic phase. At low temperatures a localised canted state (LCS) is phenomenologically equivalent to the re-entrant state or semi-spin-glass phase. The only difference lies in the appearance of a collinear structure at high temperatures, which is not expected in the LCS model. It is also noteworthy that the exchange linkage approach [2] belongs to the same phenomenology as percolation calculations and that a modern version of this approach could be based on the existence of clusters uncorrelated with the infinite magnetic network [22].

In this paper we discuss briefly the experimental techniques which provide evidence for disordered magnetic phases in ferrites and in particular LCSs. We indicate the systems where these types of phase have been found and finally we establish an experimental phase diagram.

2. Discussion

We are concerned with the properties of disordered magnetic phases and in particular LCSs. Therefore we first discuss the results of high-field magnetisation and Mössbauer

spectroscopy in a high applied field, both of which give direct evidence for a canted structure. Since the spin-glass or spin-glass-like states are demonstrated by low-field magnetisation measurements, we subsequently discuss the results obtained by these techniques. Finally we examine the results obtained by techniques which do not involve an external field, i.e. Mössbauer spectroscopy and neutron diffraction.

At the outset it is necessary to classify the systems under review since their properties depend on the species of magnetic atoms (different exchange integrals are expected) and also on the mixing of magnetic atoms within a given sublattice. We can distinguish four sorts of system:

(i) systems designated by A in table 1, with the general formulae $((M_1)_{1-x}D_x)_{(A)}[(M_3)_{1-y}D_y]_{2(B)}O_4$ where there is only one kind of magnetic atom in a sublattice (M is a magnetic atom and D a diamagnetic atom);

(ii) systems B with the general formulae $(Fe^{3+}_{1-x}D_x)_{(A)}[(M_3, M_4)_{1-y}D_y]_{2(B)}O_4$ where the A site is occupied by Fe^{3+} and the B site by a mixture of two magnetic atoms;

(iii) systems C with the general formulae $((Fe^{3+}, M_2)_{1-x}D_x)_{(A)}[(Fe^{3+}, M_4)_{1-y}D_y]_{2(B)}O_4$ where the two sites are occupied by Fe^{3+} and another magnetic atom;

(iv) finally, more complex systems D (note that there are no diamagnetic atoms in the D21 to D24 systems).

All the systems cited and the corresponding references are listed in table 1.

2.1. High-field measurements

Several systems have been the object of magnetisation measurements in high applied fields: at low temperatures the A13 [7], B12 [53], B22 [59], B31 [60], B32 [8], C23 [64] and D23 [72] systems and, as a function of temperature, the A11 [23], A13 [9, 25], A15 [31], A16 [35] and D13 [69] systems. The same trend is always observed. Beyond a certain concentration, i.e. when x exceeds a certain value, the magnetisation at low temperature does not saturate for fields up to 16 T and the value obtained at the highest fields is smaller than that expected from a collinear model. At higher temperatures, the same type of variation is observed with a decrease in the magnetisation as illustrated in figure 1. These features are strong evidence for a canted structure but it is difficult to distinguish between a LCS or a Yafet–Kittel-type structure. As a rule, two special features occur.

(i) At low and medium fields, the magnetisation does not reach a maximum at the lowest temperature but at an intermediate temperature. This may indicate a decrease in the magnetic order at low temperatures but it can also be explained by a different variation in the magnetisation of each sublattice.

(ii) Above the Néel temperature T_N determined from low-field magnetisation or susceptibility measurements, the plot of magnetisation against field shows a slight curvature, indicating that the true paramagnetic state is not reached. It is likely that some short-range order exists above T_N and that the transition from the paramagnetic to the magnetic states takes place over a large temperature range due to the occurrence of clusters coming from short range order. With decreasing temperature the clusters grow and merge into the infinite magnetic network [22].

Mössbauer spectroscopy in applied fields has been performed at low temperatures on numerous systems: A12 [24], A13 [26], A16 [36], A17 [40], A41 [47], B11 [50], B21 [54, 55], B31 [60], B32 [8], C31 [65], D21 [70], D22 [71] and D23 [73]. Concerning this

Table 1. List of systems for which compounds show LCSS or disordered magnetism from certain x-values (for classification see text).

Ions	Designation	Compound	Reference
$M_1 \equiv M_3 \equiv Fe^{3+}$	A11	$Fe_{2.5-x}Al_xLi_{0.5}O_4$	[23]
	A12	$Fe_{2.5-x}Ga_xLi_{0.5}O_4$	[24]
	A13	$Fe_{2.5-0.5x}Zn_xLi_{0.5(1-x)}O_4$	[7, 9, 25–29]
	A14	$Fe_{2.5-0.5x}Cd_xLi_{0.5(1-x)}O_4$	[30]
	A15	$Fe_{2.5-1.5x}Ti_xLi_{0.5(1+x)}O_4$	[31–34]
	A16	$Fe_2Zn_xMg_{1-x}O_4$	[35–39]
	A17	$Fe_{2-x}Al_xMgO_4$	[40]
	A18	$Fe_{2-2x}Ti_xMg_{1+x}O_4$	[16]
$M_1 \equiv M_3 \equiv Fe^{2+}$	A21	$FeAl_2O_4$, $FeGa_2O_4$	[41, 42]
$M_1 \equiv M_3 \equiv Co^{2+}$	A31	$Co_{2-x}Zn_xTiO_4$	[14, 43, 44]
	A32	$CoGa_2O_4$, $CoAl_2O_4$	[42, 45]
	A33	$Co_{1-x}Zn_xRh_2O_4$	[46]
$M_1 \equiv Mn^{2+}$, $M_3 \equiv Fe^{3+}$	A41	$Mn_{1-x}Zn_xFe_2O_4$ ($x \geqslant 0.6$)	[47, 48]
$M_1 \equiv O$, $M_3 \equiv Cr^{3+}$	A51	$Cr_{2x}Ga_{2-2x}ZnO_4$	[22, 49]
$M_3 \equiv Fe^{3+}$, $M_4 \equiv Co^{2+}$	B11	$Fe_2Co_{1-x}Zn_xO_4$ ($x \geqslant 0.4$)	[50–52]
	B12	$Fe_2Co_{1-x}Cd_xO_4$ ($x \geqslant 0.4$)	[53]
$M_3 \equiv Fe^{3+}$, $M_4 \equiv Ni^{2+}$	B21	$Fe_2Ni_{1-x}Zn_xO_4$	[54–58]
	B22	$Fe_{2-x}NiAl_xO_4$ ($x \leqslant 0.9$)	[59]
$M_3 \equiv Fe^{3+}$, $M_4 \equiv Fe^{2+}$	B31	$Fe_{3-x}Ga_xO_4$	[60]
	B32	$Fe_{3-x}Zn_xO_4$	[8]
$M_3 \equiv Ni^{2+}$, $M_4 \equiv Cr^{3+}$	B41	$Fe_{1-x}CrNiGa_xO_4$	[61, 62]
$M_2 \equiv M_4 \equiv Mn^{2+}$	C11	$Fe_2Mn_{1-x}Zn_xO_4$	[47, 63]
$M_2 \equiv M_4 \equiv Co^{2+}$	C21	$Fe_2Co_{1-x}Zn_xO_4$ ($x < 0.4$)	[50, 52]
	C22	$Fe_2Co_{1-x}Cd_xO_4$ ($x < 0.4$)	[53]
	C23	$Fe_{2-x}CoAl_xO_4$	[64]
$M_2 \equiv M_4 \equiv Ni^{2+}$	C31	$Fe_{2-x}NiAl_xO_4$ ($x \geqslant 1$)	[59, 65]
$M_2 \equiv Mn^{2+}$, $M_4 \equiv Ni^{2+}$	C41	$Fe_2Mn_{1-y-x}Ni_yZn_xO_4$	[66]
	D11	$FeCrCo_{1-x}Zn_xO_4$	[67, 68]
	D12	$Fe_{0.6}NiCr_{1-y}Al_yGa_{0.4}O_4$	[62]
	D13	$Ni_xCd_{1-x}Mn_2O_4$	[69]
	D21	$Fe_2Cu_{1-x}Mn_xO_4$	[70]
	D22	$Fe_{2-x}Cr_xCoO_4$	[71]
	D23	$Fe_{2-x}Cr_xNiO_4$	[71–73]
	D24	$Fe_{2-x}Cr_xMnO_4$	[72]

experiment, we note a short review paper [74] and a result obtained on a monocrystal [63]. Some systems have been studied as a function of temperature: A11 [23], A15 [31], A16 [37], A18 [16], A41 [48], A51 [22] and B21 [56].

In Mössbauer spectroscopy, if lines 2 and 5 of the six lines hyperfine pattern do not collapse when an external field is applied parallel to γ-rays, a canted structure must exist. From the relative areas of these lines, it is possible to deduce the mean canting angles. It is necessary to use sufficiently high fields to suppress the domains and it is advisable to increase the field up to 6 T in order to determine (or to check when the site occupation is known) the populations of the two sites.

Several general trends can be deduced from the published results.

(i) Canting within the B sites appears when the concentration x of non-magnetic atoms in the A sites is greater than about 0.3 and the mean canting angle increases with

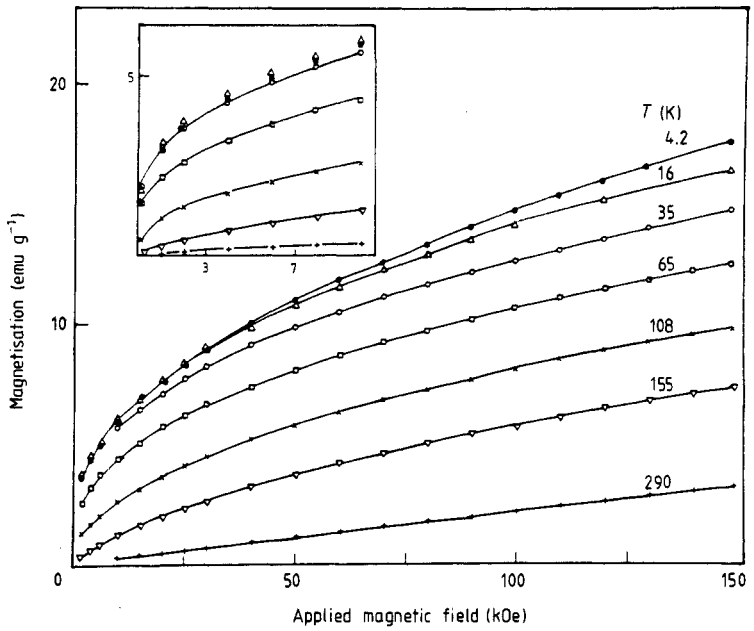

Figure 1. Magnetisation against applied field for different temperatures in the case of the A15 system with $x = 1.25$ [31].

increasing x. Canting within the A sites can also occur but only when the dilution in B sites is much higher, $y \geqslant 0.6$. However, results exist for only a few systems (A11, A15 and A17). The mean canting angle also increases with increasing y. This trend is in agreement with the LCS model [9] taking into account the usual values of intra-sublattice exchange. Therefore it is possible to find systems with only B site canting (A12, A13, A16, A18, A41, B11, B21, B31 and C31), others with only A site canting (A17) and systems where both sites are canted (A11 and A15). We observe that the third situation is not expected in the LCS model.

(ii) If the longitudinal component S_z of the canted spin is parallel to the applied field H, the mean canting angle θ decreases when H increases. If S_z is antiparallel to H, the results are not clear and it seems that θ increases slightly with increasing H (A11 and A15 systems).

(iii) In the case of strong dilution in the A sites ($x \geqslant 0.7$), some B spins have canting angles higher than 90° and therefore the population of the A sites, deduced from Mössbauer spectroscopy, is apparently higher than the actual occupancy (A13, A16, A41, B21 and B32 systems) (figure 2). The population of reversed B spins is approximately equal to the probability of finding six non-magnetic nearest neighbours although it is necessary to take into account the effect of second neighbours [8] for x near unity.

(iv) At higher temperatures, the intensities of lines 2 and 5 decrease and vanish at a temperature less than T_N (figures 2 and 3). This seems to indicate a transition from a canted structure to a collinear one. This transition is progressive, occurring over a large temperature range (figure 4).

Nevertheless, when both Mössbauer spectroscopy and high-field magnetisation measurements are performed, a discrepancy exists between the results (A11, A15 and

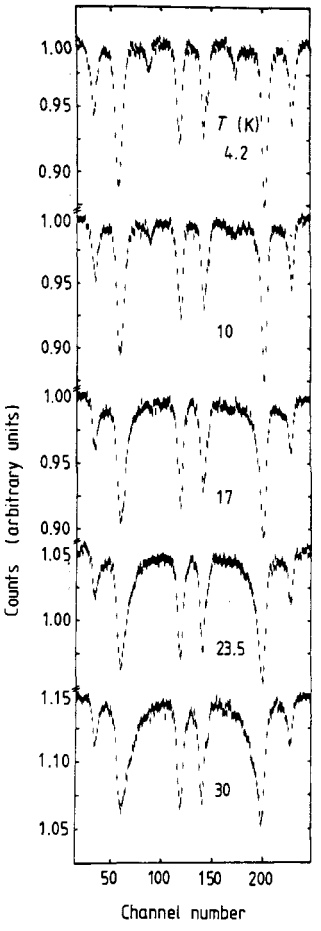

Figure 2. Temperature dependence of the Mössbauer spectra performed with a field of 8 T in the case of the B21 system with $x = 0.75$ [56].

A16 systems). Indeed, magnetisation curves do not show a collinear structure for any temperature. To resolve this discrepancy, a model has been proposed [31]. It is assumed that the transverse spin component S_t relaxes between preferential directions by a thermally activated process. The magnetisation measurements yield only the longitudinal spin component S_z when the domains are suppressed, and the relaxation does not affect the results. For Mössbauer spectroscopy in an applied field, the results depend on the value of the relaxation time τ relative to the measuring time τ_m. If $\tau \ll \tau_m$, only S_z is experienced and therefore an apparent collinear structure occurs. However, if $\tau \gg \tau_m$, Mössbauer spectroscopy sees the total spin and a canted spin structure is indicated. As τ is probably distributed and intermediate phenomena can occur when $\tau \simeq \tau_m$, the apparent transition toward a collinear structure take place progressively with temperature, as observed (figure 4). This explanation differs from the semi-spin-glass model [12] or re-entrant transition [13] in the sense that there is no sharp transition for S_t at any given temperature but only progressive freezing.

In the case of compounds with a strong A-site dilution, for which reversed B spins exist (A16, A41 and B21 systems), the same features occur. In addition, when the applied field is sufficiently high to enable the population of the two sites to be determined,

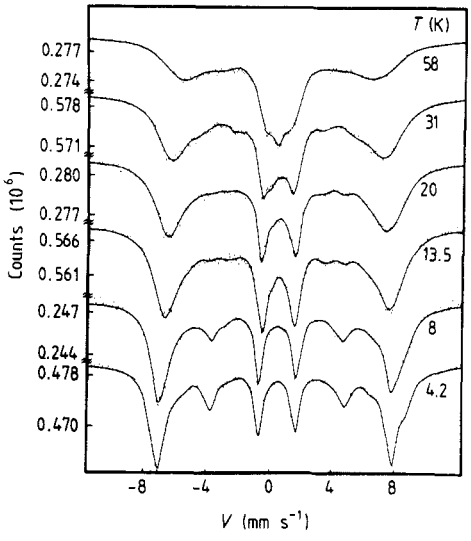

Figure 3. Temperature dependence of the Mössbauer spectra performed with a field of 1 T in the case of the A15 system with $x = 1.25$ [31].

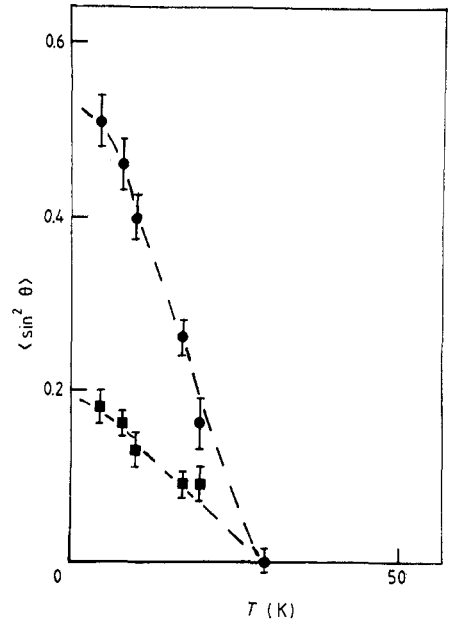

Figure 4. Temperature dependence of the mean canting angles θ_A (●) and θ_B (■) deduced from Mössbauer spectra performed with a field of 1 T in the case of the A15 system with $x = 1.25$ [31].

one observes a decrease in the population corresponding to A and B reversed sites when the temperature increases. This decrease seems to reach the actual value of the A-site population near a temperature corresponding to the collapse of lines 2 and 5, as if reversed B spins resume the normal direction. Nevertheless a significant increase in the magnetisation, resulting from a direction change of reversed B spins, does not occur with increasing temperature. Two explanations for this discrepancy are possible. If the reversed B spins are canted (the results are not clear in this matter), a significant decrease in the measured hyperfine field is expected with increasing temperature when the S_t relaxation time τ approaches τ_m. It is probable that τ for the reversed B spins is smaller than that of the normal B spins and so a decrease in the apparent A-site population is expected when the temperature increases. The same effect can be obtained if the magnetisation of the reversed B spins decreases more quickly than for the normal B spins when the temperature increases, taking into account the fact that they probably have six non-magnetic nearest neighbours. Further experiments and analysis are needed to resolve this point.

Finally we note that a Yafet–Kittel structure seems incompatible with the results, except in the case of non-diluted samples (D21, D22 and D23 systems). For a review of this case and of the triangular structure see [21].

2.2. *Low-field measurements*

Low-field measurements are often used to identify spin-glass or spin-glass-like phases in which no long-range order occurs. Thermoremanent magnetisation and frequency-dependent AC susceptibility measurements provide information on the dynamics of the

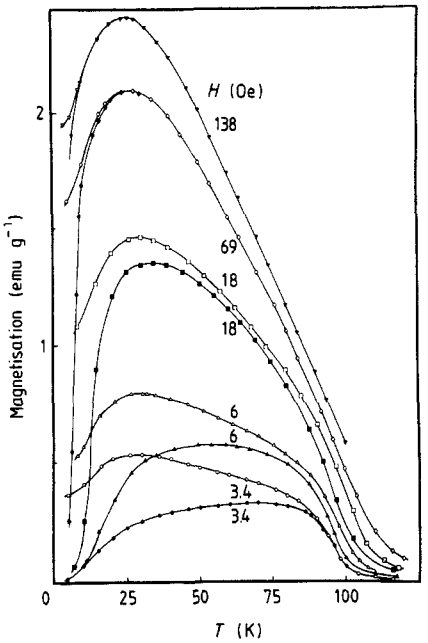

Figure 5. Temperature and field dependences of the FC (○, △, □, ◇, ▽) and ZFC (●, ▲, ■, ◆, ▼) magnetisations in the case of the A15 system with $x = 1.25$ [32].

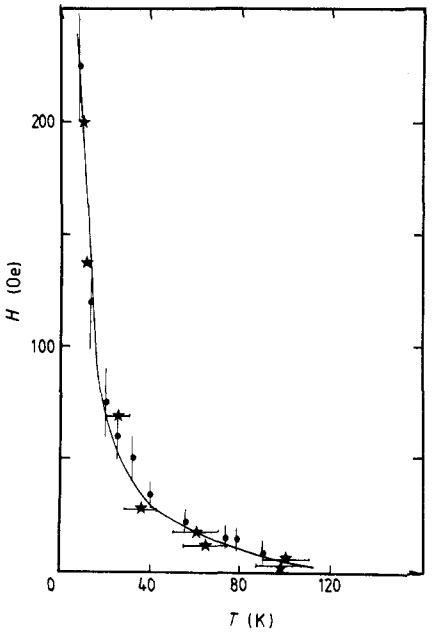

Figure 6. Branching point of FC–ZFC magnetisation (–★–) and field at which the hysteresis loop closes against temperature in the case of the A15 system with $x = 1.25$.

system. Static zero-field-cooled (ZFC) or field-cooled (FC) magnetisation measurements against field can reveal whether a true phase transition occurs. When long-range order is expected, as in LCSS, a difficulty arises since domains exist. The problem is to distinguish, in the measured susceptibility, between that part originating from domain wall movements and a possible part due to the disorder. The interpretation is never unambiguous except when direct evidence of the absence of long-range order is given by neutron diffraction. There are some features which offer a first approach to the understanding of the properties. There are also some properties which, at first sight, appear characteristic of spin-glass-like or cluster glass phases but which are not in reality a proof.

Only two systems have been the object of detailed studies: the A15 [32, 33] and A51 [49] systems. Only the first is representative of a two-sublattice system. Partial studies have been performed on other systems: ZFC and FC magnetisation and hysteresis loop measurements on A11 [23], A18 [16], A31 [43], B11 [51], B41 [61], D11 [67], D13 [69] systems, AC susceptibility on A21 [41, 42], A31 [44], A32 [45], B11, B41 and D11 systems, and thermoremanent magnetisation on A11 [23] and A31 [43] systems.

FC and ZFC magnetisation measurements seem to demonstrate strong irreversibilities (figure 5), as in spin-glass or spin-glass-like phases. The same trend is observed for all the samples studied. These irreversibilities are strongly field dependent in the whole temperature range below T_N and disappear at medium fields. Moreover the coercive field is small below T_N, as in ferrimagnets, but increases strongly at low temperatures where both S_t freezing and hysteresis loop time dependence are observed [32, 33]. In figure 6, we have represented firstly the field dependence of the branching point

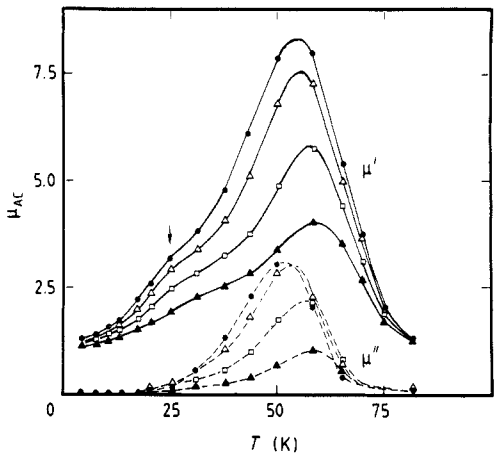

Figure 7. Temperature and frequency (●, 0.25 kHz; △, 1 kHz; □, 10 kHz; ▲, 100 kHz) dependences of the in-phase permeability μ' and out-of-phase permeability μ'' in the case of the A15 system with $x = 1.32$.

temperature of ZFC and FC magnetisation curves and secondly the temperature dependence of the field at which the hysteresis loop closes, in the case of an A15 compound with $x = 1.25$ [32, 33]. The two curves are superposed. The same features are observed in a D13 system [69] and show that the irreversibilities could only be the consequence of the variation in the hysteresis loop with temperature, an interpretation in terms of clusters or spin-glass-like phases being then inadequate.

The AC susceptibility χ_{AC} often shows intricate properties. For example, figure 7 shows the temperature and frequency dependences for Li–Ti ferrite (A15 system with $x = 1.32$). It is to be expected that the LCS will cause complex domains and domain walls that lead to complicated behaviour. Moreover, anomalies can occur in χ_{AC} at high frequencies and near T_N owing to domain wall relaxation and near the S_t freezing temperature. To relate to any phase transformation or any spin or cluster freezing, it is necessary to examine the imaginary part of χ_{AC}, which must show the same types of anomaly. Also the variation in these anomalies with frequency can give information on the dynamics of the phase transformation or the freezing. In our opinion the χ_{AC} results demonstrate the existence of a spin-glass-like phase only for the A21 and A32 systems; this is confirmed by the absence of magnetic reflections in neutron diffraction.

The thermoremanent magnetisation shows a similar variation to that obtained for a spin-glass-like phase with the natural logarithm of the thermoremanent magnetisation proportional to $\ln t$. Only in the A31 system has a stretched exponential law been observed [43]. In the A15 system with $x = 1.25$ [32, 33], the remanent magnetisation and thermoremanence exhibit two regimes: one for temperatures above 15 K and the other for temperatures below 15 K. The activation energy is the sum of two terms of which one is inversely proportional to the relaxation time of the transverse spin component. In our opinion these properties can be explained in terms of the complex structure of domains and domain walls due to LCSS. After cooling at low temperatures, S_t is frozen in an energy minimum. The energy required to move the walls is important as the energy barrier between energy minima is high. In fact, after spin rotation, S_t is not in a direction which minimises the energy and therefore the system relaxes [32, 33]. At high temperatures, the energy barrier is low and S_t relaxation is rapid. Therefore the equilibrium state is reached rapidly and the compound behaves as a normal ferrimagnet [32].

In the case of substituted ferrites, low-field measurements do not yield evidence concerning the magnetic structure. From the systems reviewed, spin-glass-like phases have been demonstrated for the systems A21, A32 and A51 by other techniques. LCSs are certain or probable in the A11, A15, A18, A31, B11 and D11 systems. It is also probable that special properties occur in the B41 and D11 systems owing to the complex mixture of magnetic ions which causes significant frustration.

2.3. Measurements without a field

In this type of measurement there is no perturbation of the magnetic state by a magnetic field. Examples are neutron diffraction (which reveals the magnetic structure and the presence of long-range order), Mössbauer spectroscopy and nuclear magnetic resonance (NMR).

Certain compositions of some systems have been the object of neutron diffraction studies (for a survey, see [75]). For the systems A21 [41], A31 with $x = 0.8$ and 1 [14, 43], A32 [45] and A51 with $x \leqslant 0.85$ [49], the absence of long-range order magnetic lines and the existence of a developed short-range order hump peaking indicate spin-glass or spin-glass-like properties. In the case of systems A13 with $x = 0.66$ [27], A15 with $x = 1.1$ and 1.32 [32], B21 with $x = 0.5$ and 0.75 [57] and B31 with $x = 0.4$ and 0.8 [60], the existence of a magnetic contribution in the neutron lines indicates long-range ferrimagnetic ordering. The absence of a sharp (200) magnetic reflection and the fact that the deduced magnetic moment (at least for one site) is clearly lower than the expected values from a collinear structure are in favour of the LCS structure. The same features are observed for the systems A31 with $x = 0$, 0.2 and 0.4 [14, 43] and D11 with $x = 0.5$ [68] but with, in addition, a broad diffuse hump at low temperatures. For the latter compound the hump disappears at a temperature well below T_N and is related to the S_t short-range correlation. In this compound, steps in the temperature dependence of the magnetic moment are observed, similar to those seen in the system A13 with $x = 0.66$ (single-crystal sample) [28]. Further experiments are required (in particular against temperature) to distinguish between a semi-spin-glass state and a LCS with S_t relaxation.

Numerous systems have been the object of Mössbauer studies without an applied field, but it is difficult to deduce pertinent results concerning the magnetic structure because the presence of relaxation complicates the interpretation of the spectra. On the other hand, in certain systems, a paramagnetic part exists well below the Néel temperature and its population increases greatly with increasing temperature. The presence of ionic spin relaxation has been clearly demonstrated in B11 [52] and B21 [56, 58] systems and seems a general feature related to LCSs. Nevertheless the model considers only longitudinal relaxation and it would be interesting to take into account the transverse spin relaxation appearing in LCSs. We feel that this improvement could explain the occurrence of the paramagnetic part and the abnormal variation in the hyperfine field with temperature. Nevertheless it seems also that near the Néel temperature, as we have explained above, clusters uncorrelated with the infinite magnetic network can occur and are responsible, to some degree at least, for the paramagnetic part.

Finally, we note a NMR experiment on the D12 system [62] which has clearly shown the existence of a canted structure.

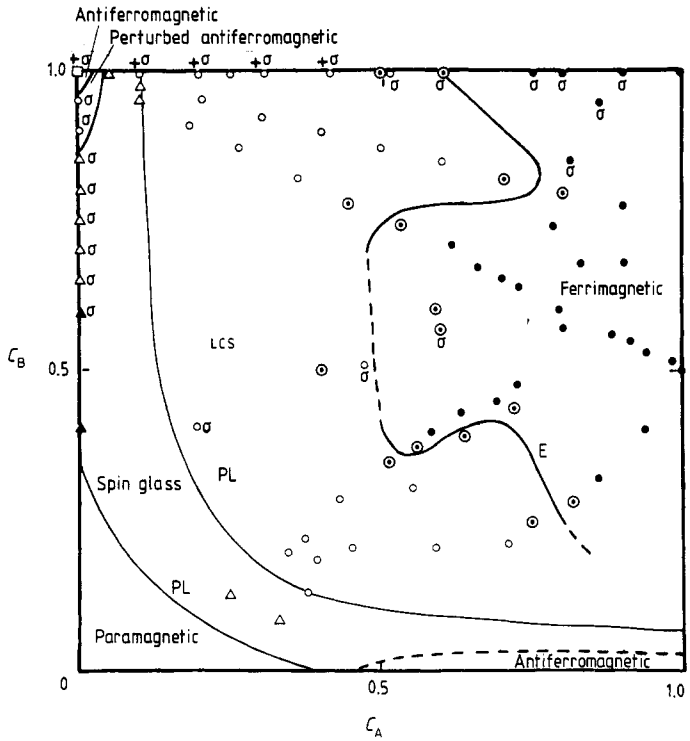

Figure 8. Experimental phase diagram for Fe^{3+} systems and analogous systems (see text): ●, ferrimagnetic order; ⊙, limiting case between ferrimagnetic order and LCSS; ○, LCS or perturbed ferrimagnetic order; △, spin-glass-like phase; ▲, spin-glass state; ○, paramagnetic phase; □, antiferromagnetic phase; σ, other systems; $+\sigma$, superposition of Fe^{3+} and other systems; lines PL, percolation limit lines (see text); line E, experimental line (see text).

3. Phase diagram

From the results that we have examined, experimental phase diagrams can be established (figures 8 and 9), in which the compounds have been mainly classified in four categories:

(i) ferrimagnetic order;
(ii) dubious cases difficult to classify in terms of ferrimagnetic order and LCSS;
(iii) LCS or perturbed magnetic order;
(iv) spin-glass or spin-glass-like phases.

We have distinguished between the directly comparable compounds with Fe^{3+} (A11 to A18 systems) (figure 8) and the systems which contain anisotropic magnetic ions: Fe^{2+} (A21 and B31), Co^{2+} (A31, A32, A33, B11, B12, C21, C22, C23, D11 and D22) and Mn^{3+} (D13) (figure 9).

For the other materials, some systems behave similar to Fe^{3+} compounds and are also indicated in figure 8: A41, A51, B21, B22, C11, C31 and C41. We note that for the two first systems there is no magnetic atom mixture but for the other systems a mixture of Fe^{3+}–Ni^{2+} and Fe^{3+}–Mn^{2+} exists. The systems B41, D12, D23 and D24 behave

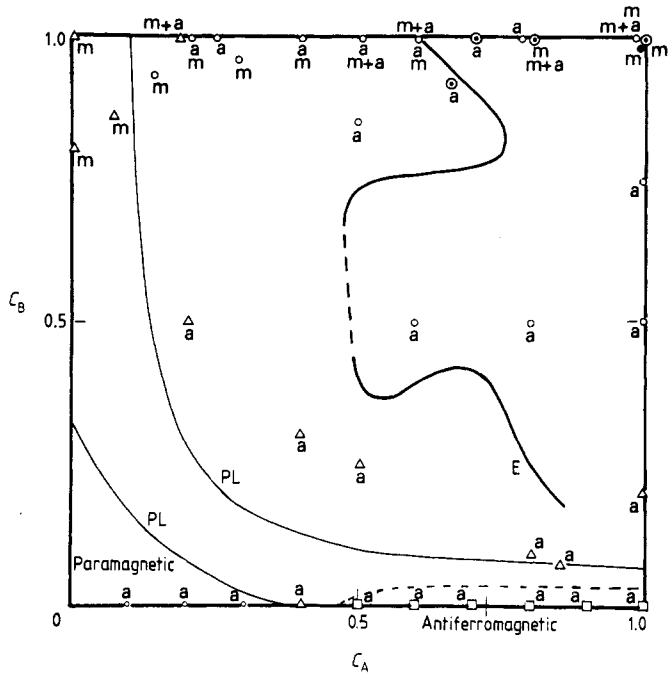

Figure 9. Experimental phase diagram for anisotropic ion systems and Cr^{3+}–Me mixtures (see text): symbols have the same meaning as in figure 8; a, anisotropic systems; m, mixture systems; m + a, mixture of anisotropic and Cr^{3+} ions in some systems.

similarly to anisotropic compounds and are a mixture of magnetic atoms with Cr^{3+} (figure 9).

The percolation limit lines (see § 1) are labelled PL in the phase diagrams.

For the Fe^{3+} compounds (figure 8), the percolation model is not in contradiction with the experimental results. Between the two percolation lines PL, spin-glass-like phases are generally obtained except in the concentration region where 'high C_B values – $C_A = 0$' (antiferromagnetic and perturbed antiferromagnetic phases). Few results are available in the spin-glass region, and no information at all for $C_B = 0$.

In figure 8, on the right of the percolation line for AB bonds, it is possible to draw an experimental line (line E) which separates the ferrimagnetic region from the LCS region. This line is only approximate because it is difficult to know precisely whether a true ferrimagnetic phase occurs or a weakly canted phase. This line E is not well defined in some concentration ranges because of the lack of experimental results. Such a lack of results also causes uncertainties in other regions of the phase diagram. For example, antiferromagnetic order can probably occur in the range '$C_B = 0, 0.5 \leqslant C_A \leqslant 1$'. In this range and for very weak C_B-values, does antiferromagnetic order persist or does a spin-glass-like state occur?

Some systems behave similarly to the Fe^{3+} compounds.

(i) The A51 (Cr^{3+} in B site) and A41 (Mn^{2+} in A site and Fe^{3+} in B site) systems have no mixture of magnetic atoms in either site. In spite of different exchange integrals, these systems behave similarly to the Fe^{3+} compounds. This indicates that the dilution of magnetic atoms is the predominant factor for obtaining the observed structures.

(ii) Certain systems have Ni^{2+}–Fe^{3+} or Mn^{2+}–Fe^{3+} mixtures. In the case of Ni^{2+}, the $(Ni^{2+}–Fe^{3+})_{BB}$ and $(Ni^{2+}–Ni^{2+})_{BB}$ exchange integrals are less negative than the $(Fe^{3+}–Fe^{3+})_{BB}$ integral [76, 77]. This leads, in a certain sense, to a decrease in the frustration. It is not therefore surprising that these systems have approximately the same properties as the Fe^{3+} systems. The same feature seems to occur for a Mn^{2+}–Fe^{3+} mixture [76] whereas in the case of Cr^{3+} the BB exchange integrals are more strongly negative [77].

In the second phase diagram (figure 9), results concerning anisotropic magnetic ions and mixtures with Cr^{3+} systems have been reported. By comparison with figure 8, a more extended spin-glass-like region and a shift to higher concentrations of the LCS region are observed. The ferrimagnetic region, observed for only some systems, is strongly reduced at around $C_B = C_A = 1$. In the case of mixtures with Cr^{3+}, the strong negative values of the Cr^{3+} exchange, and in particular the BB interactions [77], lead to an increasing frustration which destabilises the ferrimagnetic network at quite low levels of dilution.

For anisotropic magnetic ion systems, no model has been developed for random cubic anisotropy and interaction disorders. Nevertheless, we can use the prediction of the uniaxial random-anisotropy model [18]. In our case, mean values of anisotropy are expected. With increasing field, three magnetic states can occur:

(i) a correlated spin glass (CSG),
(ii) a ferromagnetic state with a wandering axis (FWA) and
(iii) a ferromagnetic state with some very weak deviations.

If coherent anisotropy exists (as for example uniaxial anisotropy due to magnetoelastic effects in amorphous ferromagnets), the field limits between the three states, which depend on the anisotropy strength, decrease with increasing coherent anisotropy. As the anisotropy is strongly temperature dependent, so too are the field limits, and it is possible to observe, at constant field, the three states as a function of the temperature.

In the anisotropic ferrite systems under review, the anisotropic magnetic ions (Mn^{3+}, Fe^{2+} and Co^{2+}) randomly occupy one site. The expected resulting anisotropy is the sum of the cubic coherent (non-random) anisotropy and the uniaxial random anisotropy following a 100- or 111-type axis. On the other hand, the CSG state is a kind of spin-glass-like phase and the FWA state is phenomenologically equivalent to the LCS, although the correlation length is not the same. Therefore the effect of the anisotropic ions is to extend the spin-glass region and to shift the LCS region. The LCS region is observed in a concentration range where ferrimagnetic order exists in the case of isotropic ions, and the spin-glass-like phase replaces the isotropic LCS case.

These experimental diagrams are quite different from the theoretical diagram in [12] and diagram in [78] based mainly on experimental results but also on theoretical considerations. Note that, for the diagram in [78], diluted samples were considered only theoretically. We think that our diagram is more realistic and takes into account the actual phase of numerous diluted samples. Some differences from the diagram in [21] also occur, essentially in the spin-glass region. For certain regions, notably antiferromagnetic and randomly canted antiferromagnetic, no pertinent experimental results are available.

Finally, we emphasise that supplementary detailed studies at low fields are required to understand the properties of domains and domain walls induced by LCSs. Also, it is clear from phase diagrams that certain concentration regions have been the object of only a few studies. The limit problems remain open and, in particular, the evolution of the LCS phase to the antiferromagnetic phase is not known.

References

[1] Guillaud C and Roux M 1949 *C. R. Acad. Sci., Paris* **228** 1110
[2] Néel L 1950 *C. R. Acad. Sci., Paris* **230** 375
Gilleo M A 1958 *Phys. Rev.* **109** 777
[3] Yafet Y and Kittel C 1952 *Phys. Rev.* **87** 290
[4] Geller S 1966 *J. Appl. Phys.* **37** 1408
[5] Nowik I 1969 *J. Appl. Phys.* **40** 5184
[6] Rosencwaig A 1970 *Can. J. Phys.* **48** 2857, 2868
[7] White G O, Edmonson C A, Goldfarb R B and Patton C E 1979 *J. Appl. Phys.* **50** 2381
[8] Dickof P A, Schurer P J and Morrish A H 1980 *Phys. Rev.* **22** 115
[9] Patton C E and Liu Y H 1983 *J. Phys. C: Solid State Phys.* **16** 5995
[10] Winkler G 1981 *Magnetic Garnets* (Braunschweig: Vieweg)
[11] Toulouse G 1977 *Commun. Phys.* **2** 115
[12] Villain J 1979 *Z. Phys.* B **33** 31
[13] Toulouse G and Gabay M 1981 *J. Physique Lett.* **42** L103
Gabay M and Toulouse G 1981 *Phys. Rev. Lett.* **47** 201
[14] Hubsch J, Gavoille G and Bolfa J 1978 *J. Appl. Phys.* **49** 1363
[15] Scholl F and Binder K 1980 *Z. Phys.* B **39** 239
[16] Brandt R A, George-Gibert H, Hubsch J and Heller J A 1985 *J. Phys. F: Met. Phys.* **15** 1987
[17] Sellmyer D J and O'Shea M J 1984 *J. Less-Common Met.* **94** 59
Sellmyer D J and Nafis S 1985 *J. Appl. Phys.* **57** 3584
[18] Chudnowsky E M, Saslow W M and Serota R A 1986 *Phys. Rev.* B **33** 251
Chudnovsky E M 1988 *J. Appl. Phys.* **64** 5770
[19] Fisher K H 1983 *Phys. Status Solidi* b **116** 357; 1985 *Phys. Status Solidi* b **130** 13
Huang C Y 1985 *J. Magn. Magn. Mater.* **51** 1
Chowdhury D 1986 *Spin Glasses and other Frustrated Systems* (Singapore: World Scientific)
Binder K and Young A P 1986 *Rev. Mod. Phys.* **58** 801
[20] Dormann J L and Nogues M 1987 *Proc. 3rd Int. Conf. Physics of Magnetic Materials* (Singapore: World Scientific) p 531
[21] Coey J M D 1987 *Can. J. Phys.* **65** 1210
[22] Saifi A, Dormann J L, Fiorani D, Renaudin P and Jové J 1988 *J. Phys. C: Solid State Phys.* **21** 5295
Dormann J L, Bhargava S C, Jové J and Fiorani D 1989 *Hyperfine Interact.* **50** 625
[23] Nogues M, Dormann J L, Maknani J, Villers G and Dumond Y 1990 *Proc. 5th Int. Conf. Ferrites* at press
[24] Kulshreshtha S K and Ritter G 1985 *J. Mater. Sci.* **20** 3926
[25] Patton C E, Edmonson C A and Liu Y H 1982 *J. Appl. Phys.* **53** 2431
[26] Abeledo C R and Frankel R B 1977 *J. Physique Coll.* **38** C1 135
Rosenberg M, Peppe P, Dey S, Patton C E and Edmonson C A 1982 *IEEE Trans. Magn.* **MAG-18** 1616
[27] Zhilyakov S M, Ivolga V V, Mal'tsev V I and Naiden E P 1977 *Sov. Phys.–Solid State* **19** 1817
[28] Zhilyakov S M, Ivolga V V, Mal'tsev V I and Naiden E P 1977 *JETP Lett.* **26** 548
[29] Gorter E W 1954 *Philips Res. Rep.* **9** 295
[30] Carter A E, Miles P A and Welch A J E 1956 *Proc. Convention on Ferrites* p 141
Rezlescu N and Condurache D 1974 *Phys. Status Solidi* a **26** K41
[31] Dormann J L, El Harfaoui M, Nogues M and Jové J 1987 *J. Phys. C: Solid State Phys.* **20** L161
[32] El Harfaoui M, Dormann J L, Nogues M, Villers G, Caignaert V and Bourée-Vigneron F 1988 *J. Physique Coll.* **49** C8 1147
[33] Dormann J L, Nogues M, Villers G, El Harfaoui M and Seqqat M 1989 *Proc. 5th Int. Conf. Ferrites* at press
[34] Nogues M, Dormann J L, Perrin M, Simonet W and Gibart P 1979 *IEEE Trans. Magn.* **MAG-15** 1729
Dormann J L, Merceron T and Nogues M 1982 *Proc. Int. Conf. Applications of the Mössbauer Effect* (Jaipur: Indian National Science Academy) p 193
[35] Nogues M, Dormann J L, Villers G, Zemirli M, Varret F and Teillet H J unpublished
[36] Ligenza S, Lukasiak M, Kucharski Z and Suwalski J 1983 *Phys. Status Solidi* b **117** 465
[37] Zemirli M, Greneche J M, Varret F, Lenglet M and Teillet J 1988 *J. Physique Coll.* **49** C8 917
Zemirli M 1988 *Thesis* Le Mans
[38] Joshi H H and Kulkarni R G 1986 *J. Mater. Sci.* **21** 2138
[39] Hastings J M and Corliss L M 1956 *Phys. Rev.* **102** 1460
[40] De Grave E, Govaert A, Chambaere D and Robbrecht G 1979 *Physica* B **96** 103

Sundararajan M O, Narayanasamy A, Nagarajan T, Häggström L, Swamy C S and Ramanujachary K V 1984 *J. Phys. C: Solid State Phys.* **17** 2953
[41] Soubeyroux J L, Fiorani D, Agostinelli E, Bhargava S C and Dormann J L 1988 *J. Physique Coll.* **49** C8 1117
[42] Agostinelli E and Fiorani D 1987 *Magnetic Excitations and Fluctuations* vol II (Berlin: Springer) p 55
[43] Hubsch J and Gavoille G 1982 *Phys. Rev.* B **26** 3815
[44] Srivastava J K, Ramakrishnan S, Maraté V R, Chandra G and Vijayaraghavan R 1987 *J. Appl. Phys.* **61** 3622
[45] Soubeyroux J L, Fiorani D and Agostinelli E 1986 *J. Magn. Magn. Mater.* **54–7** 83
[46] Fiorani D and Viticoli S 1980 *J. Phys. Chem. Solids* **41** 959, 1041
Fiorani D, Lapiccirella D and Viticoli S 1980 *J. Magn. Magn. Mater.* **15–8** 1311
[47] Morrish A H and Clark P E 1975 *Phys. Rev.* B **11** 278
[48] Morrish A H and Schurer P J 1977 *Physica* B **86–8** 921
[49] Fiorani D, Viticoli S, Dormann J L, Tholence J L, Hammann J, Murani A P and Soubeyroux J L 1983 *J. Phys. C: Solid State Phys.* **16** 3175
Fiorani D, Dormann J L, Tholence J L and Soubeyroux J L 1985 *J. Phys. C: Solid State Phys.* **18** 3053
[50] Petitt G A and Forester D W 1971 *Phys. Rev.* B **4** 3912
[51] Muraleedharan K, Srivastava J K, Marathe V R and Vijayaraghavan R 1985 *J. Phys. C: Solid State Phys.* **18** 5355
[52] Bhargava S C and Iyengar P K 1972 *Phys. Status Solidi* b **53** 359
[53] Sattar Mohamed A A, Ghani Awad A A, Guillot M and Marchand A 1986 *Adv. Ceram.* **15** 305
[54] Leung L K, Evans B J and Morrish A H 1973 *Phys. Rev.* B **8** 29
Clark P E and Morrish A H 1973 *Phys. Status Solidi* a **19** 677
[55] Piekoszewski J, Suwalski J and Dabrowski L 1977 *Acta Phys. Pol.* A **51** 179
[56] Bhargava S C and Zeman N 1980 *Phys. Rev.* B **21** 1717, 1726
[57] Satya Murthy N S, Natera M G, Youssef S I, Begum R J and Srivastava C M 1969 *Phys. Rev.* **181** 969
[58] Bhargava S C, Morup S and Knudsen J E 1976 *J. Physique Coll.* **37** C6 93
[59] Bara J J, Pedziwiatr A T, Stanik Z M, Szytula A, Todorovic J, Tomkowicz Z and Zarek W 1977 *Phys. Status Solidi* a **44** 325
[60] Dehe G, Suwalski J, Wieser E and Kabish R 1981 *Phys. Status Solidi* a **65** 669
[61] Srivastava J K, Jehanno G, Muraleedharan K, Kulkarni J A, Marathé V R, Darshane V S and Vijayaraghavan R 1987 *J. Magn. Magn. Mater.* **67** 43
Srivastava J K, Jehanno G and Sanchez J P 1987 *Phys. Lett.* **121A** 322
Srivastava J K, Ramakrishnan S, Nigam A K, Chandra G, Vijayaraghavan R, Srivinas V, Hammann J, Jehanno G and Sanchez J P 1988 *Hyperfine Interact.* **42** 1079
[62] Srivastava J K, Le Dang K and Veillet P 1986 *J. Magn. Magn. Mater.* **54–7** 1341; 1986 *J. Phys. C: Solid State Phys.* **19** 599
[63] Stadnik Z M and Kawai Y 1984 *J. Phys. Soc. Japan* **53** 2761
[64] Aragones J, Fert A, Ferrer N, Schmidt M C, Tejada J and Font-Altaba M 1982 *Phys. Chem. Minerals* **8** 206
[65] Kulshreshta S K 1986 *J. Mater. Sci. Lett.* **5** 638
[66] Bara J J, Bogacz B F and Danilkiewicz M I 1986 *Hyperfine Interact.* **28** 663
[67] Muraleedharan K, Srivastava J K, Marathé V R and Vijayaraghavan R 1985 *J. Phys. C: Solid State Phys.* **18** 5897; 1986 *Solid State Commun.* **60** 485
[68] Chakravarthy R, Madhav Rao L, Paranjpe S K, Kulshreshtha S K, Soper A K and Howells W S 1988 *J. Physique Coll.* **49** C8 1113
[69] Bhandage G T, Noguès M and Dormann J L unpublished
[70] Janicki J, Pietrzak J, Porebska A and Suwalski J 1982 *Phys. Status Solidi* a **72** 95
Narayanasamy A and Häggström L 1983 *J. Phys. C: Solid State Phys.* **16** 591
[71] Hauet A, Teillet J, Hannoyer B and Lenglet M 1987 *Phys. Status Solidi* a **103** 257
[72] Jacobs I S 1960 *J. Phys. Chem. Solids* **15** 54
[73] Chappert J and Frankel R B 1967 *Phys. Rev. Lett.* **19** 570
[74] Morrish A H 1981 *Proc. 3rd Int. Conf. Ferrites* (Tokyo: Center for Academic Publication) p 153
[75] Madhav Rao L 1989 *Proc. 5th Int. Conf. Ferrites* at press
[76] Motida K and Miyahara S 1970 *J. Phys. Soc. Japan* **28** 1188
[77] Blasse G 1964 *Philips Res. Rep. Suppl.* **19** 1
[78] Poole C P and Farach H A 1982 *Z. Phys.* B **47** 55